

Design and fabrication of miniature relay matrix and investigation of electromechanical interference in multi-actuator systems

著者	桑野 博喜
journal or publication title	IEEE Workshop on Micro Electro Mechanical Systems, 1994, MEMS '94, Proceedings
volume	1994
page range	313-318
year	1994
URL	http://hdl.handle.net/10097/46390

doi: 10.1109/MEMSYS.1994.555829

DESIGN AND FABRICATION OF MINIATURE RELAY MATRIX AND INVESTIGATION OF ELECTROMECHANICAL INTERFERENCE IN MULTI-ACTUATOR SYSTEMS

Hiroshi HOSAKA and Hiroki KUWANO

*Interdisciplinary Research Labs., Nippon Telegraph and Telephone Corp.
3-9-11 Midori-cho, Musashino-shi, Tokyo 180, Japan*

ABSTRACT

An 8x8 matrix relay is developed by using microsystem design and conventional machining technology. The prototype has a multilayered planar structure and 64 electromagnetic bistable switches. The system size, 28 x 32 x 7 mm, is about one tenth that of conventional relays in volume. The actuator forces generated by the spiral spring and the electro- and permanent magnets are theoretically analyzed and the results agree well with experiments. The mechanical and magnetic interference between switch actuators and the electrostatic interference between signal lines is also theoretically analyzed. The contact force is proportional to the square of the device length, the mechanical and electrical interference are independent of the length, the electrostatic interference is proportional to the length, and the limit of miniaturization is one tenth the size of the prototype.

INTRODUCTION

Mechanical switches are used in many information processing and communication systems because their on-resistance is lower than that of semiconductor switches and their off-resistance and transmission frequency are higher. Reducing their size has been a major objective - they are now about one tenth the size they were ten years ago. However, miniaturization by using conventional machining technology is reaching its limit and a new breakthrough technology is required. We previously proposed applying microelectromechanical system (MEMS) technology to mechanical relays[1]. Since a MEMS is small and its fabrication process is special, it is suitable for integration and excellent for high-speed movement. However, as a result, they cannot generate high power or be made with complicated structures. On the other hand, signal processing relays handle information and thus do not require high output power. Because their movement is only on and off, their structure is simple, so they can be easily manufactured using MEMS technology. Furthermore, micromachining of relays makes it possible to combine them with other semiconductor electronic components and to use low-cost batch processing.

There are two typical actuators for microsystems: electrostatic and magnetostatic. We think the latter are more practical because their efficiency is little affected by dust and they can be driven by common low-cost controllers. They can also be used to make self-latching relays by using a permanent magnet, which greatly reduces control power. For these reasons, we selected a magnetostatic actuator for our relay.

Earlier research into microrelays, Petersen[2], Sakata[3] and Ozawa[4] developed electrostatic relays and the authors developed a magnetostatic relay[1], focused only on single switches. Integrated or multi-actuator switches were

not studied.

We have developed an 8x8 self-latching relay matrix by using conventional machining technology to clarify the structure needed for integrating microrelays. The prototype is also targeted at usage in actual telephone networks. Its basic structure is a multilayered planar one, which is popular in MEMS design. The actuator force and electromechanical interference between actuators and between signal cables were analyzed by using the finite element method (FEM) and approximate formulas. The results were used to obtain an optimum design. The resulting relay matrix is about one tenth the volume of conventional ones. This paper describes the design and performance of the relay matrix and discusses the limitations on device size.

BASIC STRUCTURE

Basically, micromachining can be used to fabricate only multi-layered planar structures. This structure is suitable for reducing the size of conventional machines, since it is easily processed and assembled. In our prototype, the contact springs are made of sheet metal and all the components are assembled from one side, which is a layered structure. Also the spring plates and circuit boards are used in common, to reduce the number of components by utilizing a special feature of matrix switches.

Figure 1 shows an exterior view of the prototype and Fig. 2 shows its internal structure. This device can connect any of the eight input lines to any of the eight output lines through 64 independent switches. It is about one tenth the size of commercial relays - it is 28 x 32 x 7 mm. The switches are 3 mm apart. The contact springs have a spiral shape and are 2.5 mm in diameter. Each set of eight springs is fabricated from one stainless steel plate by chemical etching. Under the springs, there are 64 electromagnets, a printed board, and 90 connector pins. The pins are arranged close to the electromagnets to simplify the circuit pattern. A controlled current flows through the electromagnet core and spring plate and connects to the outer circuits via the pins. The spring plate acts both as a structural beam and electrical conductor, and the electromagnet core acts both as a magnetic and electrical conductor. To meet frequent requirement that signal relays have a self-latching function to reduce control power, a permanent magnet is fixed to each spring. By adjusting the magnetic and springback forces, both open and closed positions can be set to a stable state.

ACTUATOR DESIGN AND PERFORMANCE

Contact spring

Each contact actuator consists of a spiral spring and magnets. The spring is made of three spiral beams, as

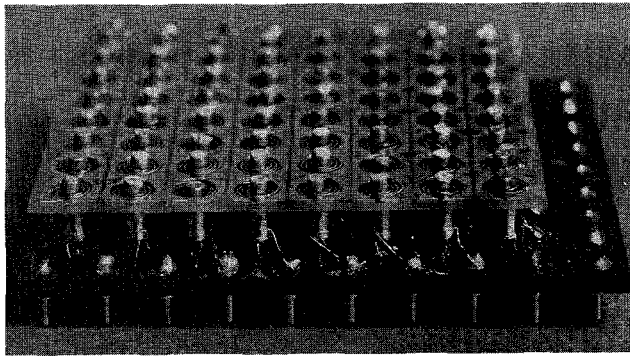


Fig. 1. Appearance of prototype.

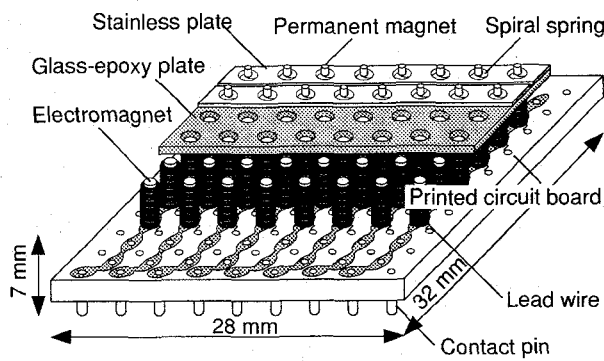


Fig. 2. Structure of prototype.

shown in Fig. 3. This structure is particularly suited for miniaturization because it is vertically flexible so a large deflection can be obtained, it is symmetric and thus is not affected by residual stress, and it is rigid in all directions other than vertical and thus its deflection is not affected by assembly error. The spring dimensions depend on manufacturing limitations: the outer radius, inner radius, beam width, and thickness are 1.25 mm, 0.5 mm, 0.1 mm, and about 0.04 mm, respectively.

To analyze the contact force generated by the actuator, we first calculated spring rigidity k_s and then compared the results with the experimental ones. In the calculation, we used an approximate formula for the helical conical spring (1)[5] and the more precise FEM.

$$k_s = \frac{12GI_p(r_o-r_i)}{\Theta(r_o^4-r_i^4)} \quad (1)$$

where G is the shearing modulus, I_p is the polar moment of inertia, and Θ is the spiral angle. In the experiment, a prototype with its permanent magnet removed was put on an electronic balance, a needle was pressed against the spring by using a microstage, and the weight increment was measured.

The calculated and measured static rigidities are shown in Fig. 4. The FEM results agree well with the experimental ones for deflections under 0.2 mm. This is because the spring is made by etching and does not have elements that add uncertainty such as bolted joints. For deflections larger than 0.2 mm, the slope of the experimental data increases slightly and the error increases to 15%. This is because the effect of nonlinearity caused by large deflection

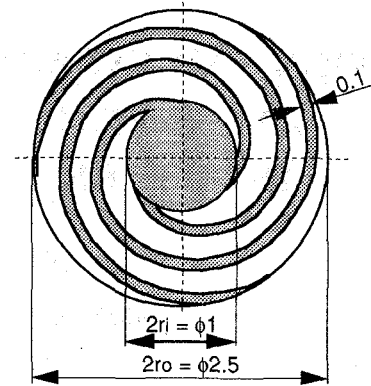


Fig. 3. Spiral spring.

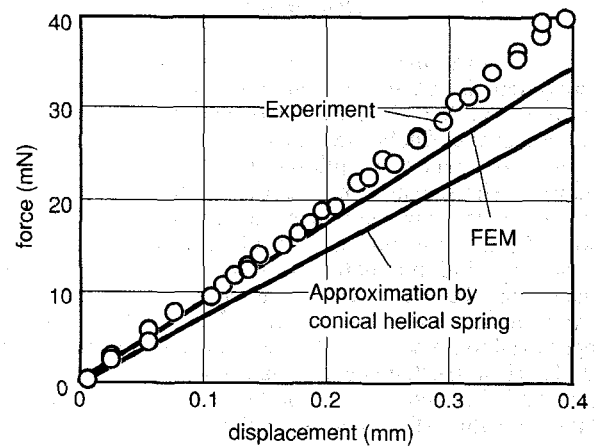


Fig. 4. Static rigidity of spiral spring.

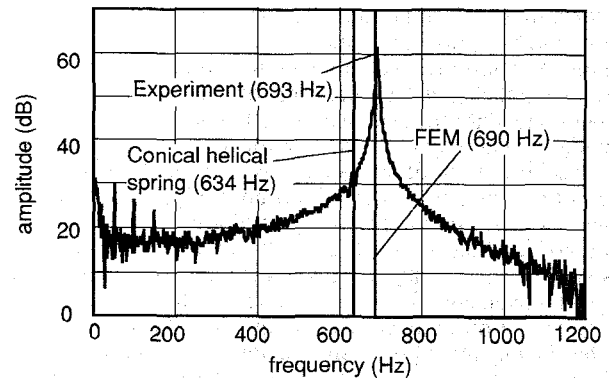


Fig. 5. Frequency response of a spiral spring.

appears in the experiment, while it was not considered in the analysis. The rigidity as calculated by approximate formula is a little smaller than the FEM results and the error from experiment is about 25%. This is because the actual boundary condition for the inner and outer radius is a fixed condition, but in Eq. (1) the boundary condition for torsion is assumed to be free, and the effect of this difference is large for springs with a small spiral angle.

We next compared the experimental and calculated frequency response in the prototype. In the approximate formula, a third of the spring mass and the permanent magnet mass are concentrated in the spring center. In the experiment, the permanent magnet was accelerated by the electromagnet and the vibration was measured with a non-

contact optical sensor. The vibration amplitude was less than 0.1 mm. The results are shown in Fig. 5. The first resonant frequency as obtained by approximate formula, FEM, and experiment are 634 Hz, 690 Hz, and 693 Hz, respectively, and the maximum error for each is less than 10%. These static and dynamic analyses show that the mechanical characteristics of spiral springs can be calculated with errors of less than 25% and 15% by using an approximate formula and FEM, respectively.

Electro- and permanent magnets

In the latching matrix switch, only a few actuators are driven at a time by using a pulse current. This means we can apply a large current to the electromagnetic coil. We therefore adopted a structure in which efficiency is low but which is easily assembled: a straight solenoid is used for the electromagnet. The number of coil turns is only 100 because our final target is a thin-film coil actuator which precludes many turns. The magnetic core is made of mild steel and is 1 mm in diameter. A rare earth permanent magnet is used with a remanence of 12.8 kG. It is 1 mm in diameter and 0.7 mm high, as determined by manufacturing limitations.

We analyzed the magnetic force and compared the results with the experimental ones. A two-dimensional FEM program is used in the calculation since the system is axisymmetric. Magnets ten times larger than that of the prototype were used in the experiment to increase measurement accuracy. A non-ferrotic film was placed between the electro- and permanent magnets and the magnets were removed by using a spring weight scale and the force at the moment of separation was measured. The relationship between the magnet gap and the force is shown in Fig. 6. When the coil current was 0, the force was 10 N for a gap of 1 mm and 2 N for a 4-mm gap in both experiment and calculation. When a coil current of ± 500 AT was applied, the force varied 1 ~ 5 N both in experiment and calculation. These results show that the magnetic force can be evaluated quantitatively by using numerical analysis.

Spring-magnet system

A self-latching switch requires a contact actuator with a bistable function. That is, when the contacts are closed, the permanent magnet force is greater than the springback force, and when the contacts are open, the condition is reversed. Using the same analytical methods described in the previous sections, we found that this condition is satisfied when the initial contact gap is 0.4 mm. The relationship between actuator force and the contact gap is shown in Fig. 7. The force is positive or negative for gaps over or under 0.03 mm, which means that the bistable mechanism functions correctly. The experimental data are also shown in Fig. 7 and they agree well with calculation. To close or open the contacts, a current pulse is applied to the coil. To open a closed contact, the electromagnet force should be positive and larger than the maximum negative force in Fig. 7: -10 mN. To close an open contact, the force should be negative and larger than the maximum positive force: 15 mN. The current amplitude is determined by the same analysis as in Fig. 6: we found the minimum current is 0.5 A. The relationship between the coil and controlled currents is shown in Fig. 8. The coil current is pulsed and has an amplitude of 0.6 A. The output is exactly controlled by the input, which means the self-latching switch functions as designed.

We estimate the limit of miniaturization from the viewpoint of contact force. When the device dimensions are reduced proportionally, the springback force is decreased in proportion to the square of the device length. Electro- and permanent magnet forces also decrease in proportion to the

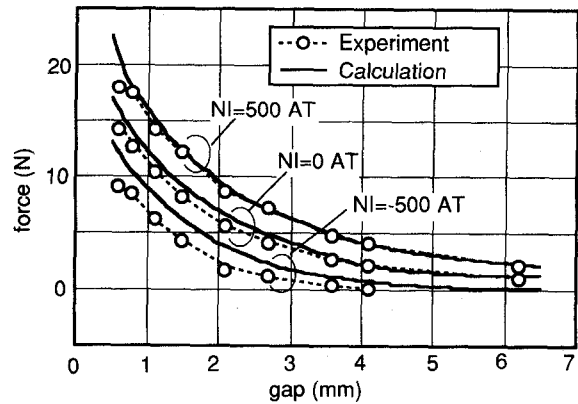


Fig. 6. Magnetic force between electro- and permanent magnets in enlarged model

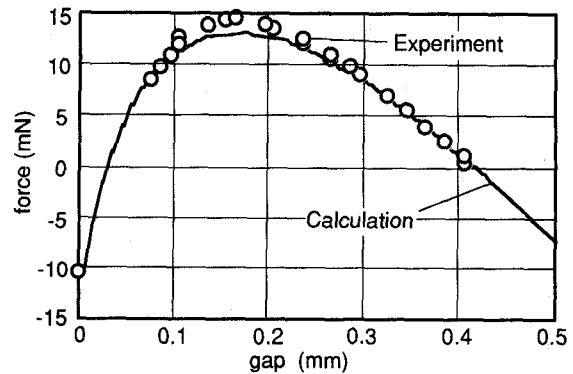


Fig. 7. Relationship between force and gap of spring-magnet system.

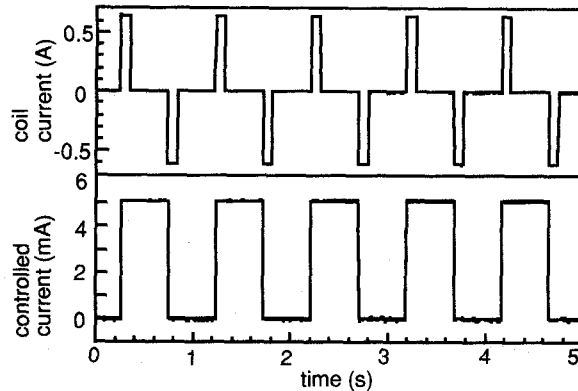


Fig. 8. Bistable switching characteristics of prototype.

square of the length when the coil current is proportional to the length. Total actuator force is thus proportional to the square of the device length. We previously reported [6] that the least contact force that gives stable contact resistance is about 0.1 mN. When we estimate the contact force by using the data in Fig. 7, 10 mN, the limit of miniaturization is about one tenth the size of the prototype as shown in Fig. 9. At this limit, the size of each actuator is 0.3 mm, which is about the same as the electromagnetic microactuator we previously developed [7].

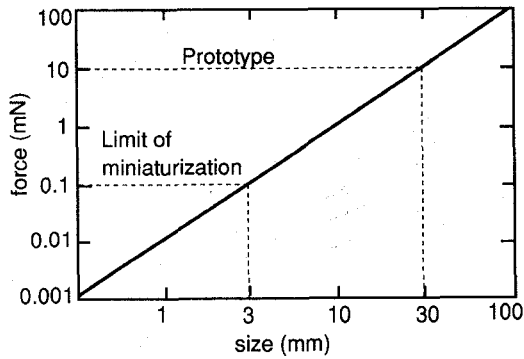


Fig. 9. Relationship between 8x8 relay size and contact force.

INTERFERENCE ANALYSIS

When a relay device is miniaturized and integrated, the actuators and signal lines are closer together, which can cause switching errors. In this section, we discuss mechanical, magnetostatic, and electrostatic interference.

Mechanical interference

Since each set of eight contact springs is made from a single stainless steel plate, vibration caused by contact activation propagates through the plate, moving the other actuators. To simplify the analysis, we neglect contact closing time in the activated contact, plate and spring inertia, and magnetic force.

Our analytical model of mechanical interference is shown in Fig. 10. Actuator o is activated and its permanent magnet is pulled down by the electromagnet. Movement of the i 'th permanent magnet is denoted by x_i and is measured from the terminal state after vibration ceases. The equation of motion for permanent magnets is given by Eq. 2 and the initial condition is given by Eq. 3:

$$m\{\ddot{x}\} + [K]\{x\} = \{0\}, \quad [K] = (k_s^l[I] + [K']^{-1})^{-1} \quad (2)$$

$$x_i(0) = \frac{c_{i,o}d}{c_{o,o} + k_s^{-1}}, \quad (3)$$

where $\{x\}$ is magnet movement, $[C]$ is the stainless beam compliance matrix, $[K']$ is the stiffness matrix of the beam with the o 'th contact spring, k_s is contact spring stiffness, m is permanent magnet mass, d is initial gap, and symbols with a suffix are matrix components.

Equations (2) and (3) are solved numerically for a system similar to the prototype, but the glass epoxy plate is cut into strips the same width as the stainless plate. The calculated results are shown in Fig. 11, where matrices $[C]$ and $[K']$ are calculated by FEM and the initial contact gap is 0.4 mm. The vibration amplitude is larger for springs closer to the activated contact: $o=4$. The largest amplitude (0.1 mm), however, is much smaller than the initial gap. This means that the switching errors do not occur. We also found that only the single mode is dominant in vibrations with a frequency almost the same as the resonance of the spring-magnet system. We next calculated the maximum amplitude of the prototype. The deflection is less than 0.014 mm, which is even smaller than the previous case. This is because the glass epoxy plate is not cut and it has large rigidity. Also the case where the glass epoxy plate is not

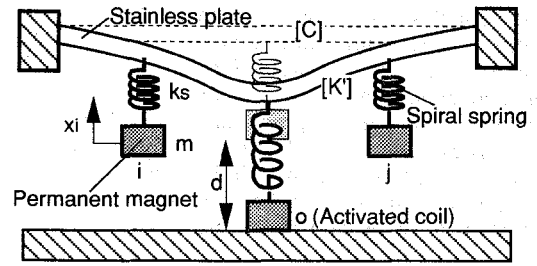


Fig. 10. Analytical model of mechanical interference.

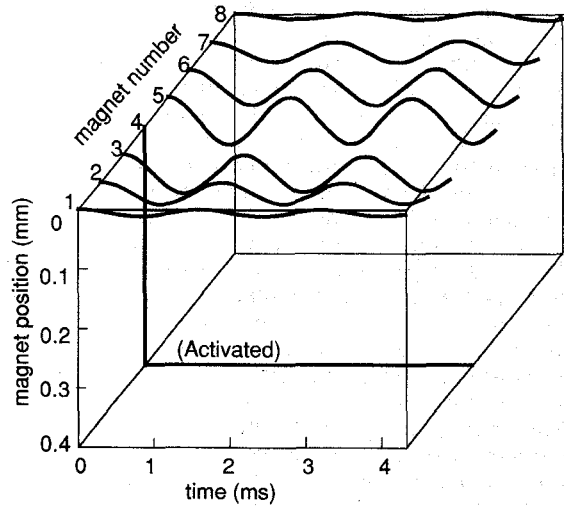


Fig. 11. Vibration of contact springs fixed to glass-epoxy beam.

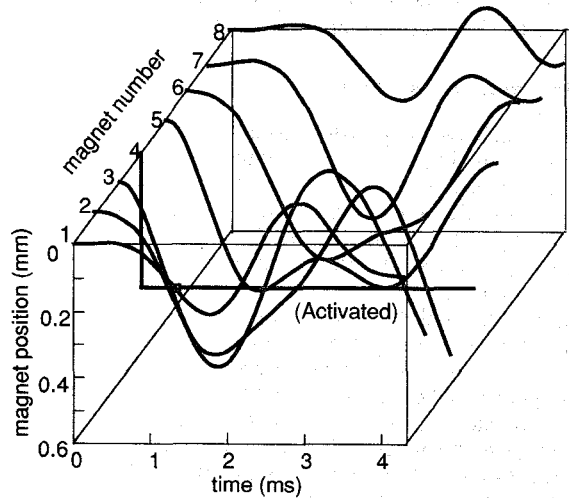


Fig. 12. Vibration of contact springs without glass-epoxy plate.

used is calculated. The results are shown in Fig. 12. In this case, the vibration pattern is complicated because the beam stiffness is small. The maximum deflection is about 0.6 mm, which means that switching errors occur.

Next we will examine the relationship between device size and mechanical interference. The vibration amplitude is determined by Eqs. (2) and (3). It depends only on the ratio of spring and beam stiffness and the initial gap when the time

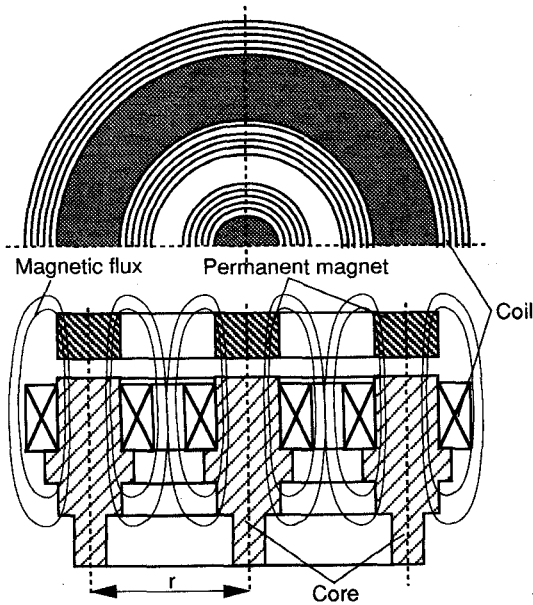


Fig. 13. Analytical model of magnetic interference.

scale is correctly adjusted. Thus, when we reduce the device size proportionally, the ratio of maximum deflection to the initial gap is independent of the size, and the mechanical interference is constant.

Magnetostatic interference

Since the actuator is magnetically an open circuit, a considerable amount of magnetic flux can leak into an adjacent actuator and cause a switching error. In this section, we will examine the case where four contacts surrounding a center contact close at the same time and calculate the closing force working on the center permanent magnet. To simplify the analysis, we use the analytical model shown in Fig. 13 in which the center actuator is surrounded by a ring-shaped actuator. This system is axisymmetric, so its force can be solved by a two-dimensional FEM. In this model, the permanent and electromagnet lengths increase as the ring diameter, i.e., the distance between actuators, increases. This does not match our requirement that the same actuator is used and only the distance between actuators is varied. We therefore decrease the remanence of the permanent magnet and the coil current of the electromagnet so that the magnetic motive force is the same as that of the four peripheral actuators. The magnetic field at the center generated by the permanent magnet and the coil is therefore almost the same as in the actual case.

The calculated results are shown in Fig. 14. The vertical axis is the force working on the center magnet when the current (a) flows only in the center coil, (b) flows only in the peripheral coil, and (c) does not flow. The horizontal axis shows the distance between actuators, i.e., the ring radius. The minimum distance where the peripheral and center coils touch is 2 mm. In all cases, force changes as the distance changes, which means the peripheral actuators affect the center one. However, the change is almost negligible when the distance is larger than 3 mm. The contact closing force generated by the center electromagnet is given by the difference between curves (a) and (c). The force generated by the peripheral one is given by (b) and (c). When the two forces are close, a switching error will occur. We therefore plotted a force ratio of (b)-(c) to (a)-(c) (Fig. 15). This ratio increases as the distance decreases, meaning that the

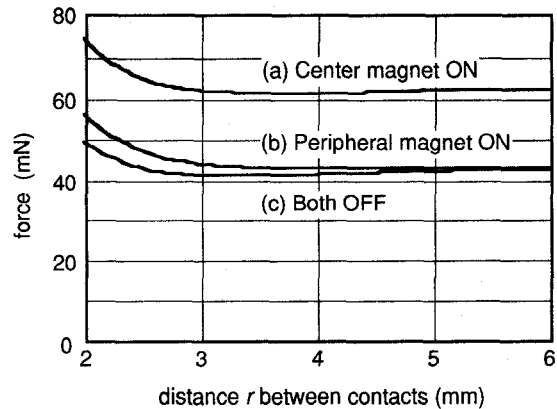


Fig. 14. Relationship between magnetic force and actuator distance.

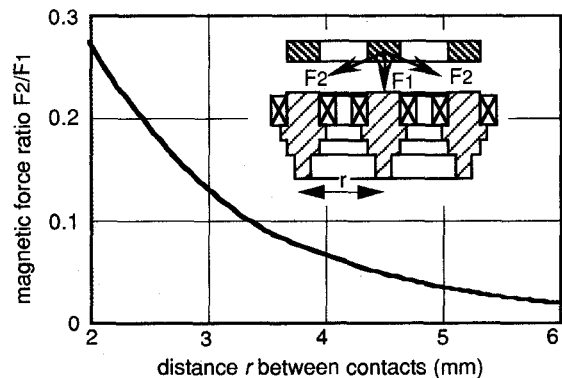


Fig. 15. Relationship between magnetic force ratio and contact distance.

probability of a switching error increases. The ratio is not large, however, and interference does not matter in a practical sense especially when the gap is larger than 3 mm. In fact, we did not observe any errors in the prototype in which the distance is 3 mm.

Magnetostatic interference is defined by the ratio of the magnetic forces generated by the peripheral and center electromagnets. Since both forces are proportional to the square of the device size, interference is independent of size.

Electrostatic interference

The signal lines are fairly densely arranged so parasitic capacitance between them can cause cross talk. In the prototype, the most critical part is the stainless plate, which has a gap of 0.2 mm. A cross sectional view of our analytical model is shown in Fig. 16. Parasitic capacitance per unit length C' is given by

$$C'[\text{pF/cm}] = C'_1 + C'_2, \quad C'_1 = \frac{\epsilon_1 K_1}{7.2\pi}, \quad C'_2 = \frac{K_2}{7.2\pi}, \quad (4)$$

where ϵ_1 is the relative permittivity of glass epoxy ($\epsilon_1 = 4.5$) and K_1 and K_2 are constants determined by a/c and b/a [8]. The size of our prototype dictates that, $K_1 = 1.5$, $K_2 = 3.2$, and $C' = 0.44$ pF/cm. By multiplying plate length 30 mm by C' , total capacitance C is 1.33 pF. The measured capacitance of the prototype is 1.5 ~ 2.8 pF, which is about the same as the calculation.

We can calculate the cross talk by using the aforementioned capacitance. We assume the prototype is used in a telephone network and the terminal resistance is 600Ω . The equivalent circuit is thus that in Fig. 17 and the cross talk is given by I_2/I_1 .

$$\frac{I_2}{I_1} = \frac{R}{R + 2/C\omega} \quad (5)$$

When we assume signal frequency ω is that of a digital network (150 kHz), I_2/I_1 is $1/2500$. This means cross talk is almost negligible in normal usage.

Since b/a and a/c are independent of size, C' is constant and total capacitance C is proportional to size. Resistance R and frequency ω are determined by the user application and are independent of device size. Therefore I_2/I_1 is almost proportional to size because R is much smaller than $2/C\omega$. For example, at the limit of miniaturization given in a previous section, I_2/I_1 is $1/25,000$.

CONCLUSION

An 8x8 matrix relay, about one tenth the size of conventional relays, was developed by using microsystem design and conventional machining technology. The relay has 64 electromagnetic bistable switches. Analysis of switch actuator performance and the interference between switches by FEM and by approximate formulas showed that the contact force is proportional to the square of device size, that mechanical and electrical interference are independent of size, that electrostatic interference is proportional to size, and that the limit of miniaturization is about one tenth the size of the prototype. Results from this research will greatly contribute to the design of integrated microrelay systems.

REFERENCES

- [1] H. Hosaka, H. Kuwano and K. Yanagisawa, "Electromagnetic microrelays, concept and fundamental characteristics", Proc. IEEE MEMS'93 Workshop, 1993, pp. 12-17.
- [2] K. E. Petersen, "Dynamic micromechanics on silicon: technique and devices", IEEE Trans. Electron Devices ED-25, 10, 1978, pp. 1241-1250.
- [3] M. Sakata, "An electrostatic microactuator for electro-mechanical relay", Proc. IEEE MEMS'89 Workshop, 1989, pp. 149-151.
- [4] K. Ozawa, "Electrostatic microrelay", Machine Design, 34, 15, 1990, pp. 70-73 (in Japanese).
- [5] E. A. Avallone, editor, "Standard handbook for mechanical engineers", McGraw-Hill, New York, 1987, p. 8-74.
- [6] H. Hosaka, H. Kuwano, K. Yanagisawa and S. Hanno, "Development of electromagnetic microrelay and its performance", Technical Report of IEICE, EMD93-19, 1993, pp. 1-6 (in Japanese).
- [7] K. Yanagisawa, A. Tago., T. Ohkubo and H. Kuwano, "Magnetic micro-actuator", Proc. IEEE MEMS'90 Workshop, 1990, pp. 120-124.
- [8] E. Tsunashima, "Design and fabrication of printed circuit", Seibundo-Shinkosha, Tokyo, 1964, p. 206 (in Japanese).

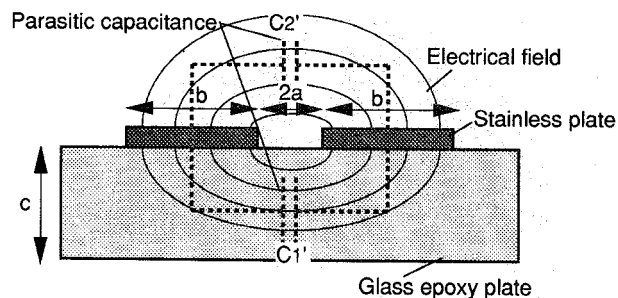


Fig. 16. Analytical model of electrostatic interference.

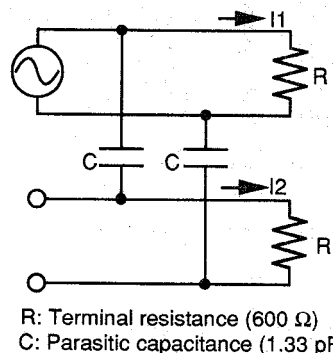


Fig. 17. Analytical model of crosstalk.